

Synthesis, Structure, and Magnetic Properties of a Novel Mixed-Valence Copper(I/II) Phosphate, Cu_2PO_4

Kristen M. S. Etheredge and Shiou-Jyh Hwu*,†

Department of Chemistry, Rice University, P.O. Box 1892, Houston, Texas 77251

Received April 26, 1995[⊗]

Via phase compatibility studies, a novel mixed-valence copper(I/II) phosphate, Cu_2PO_4 , has been isolated from a direct reaction of Cu_2O , $\text{Cu}^{\text{II}}\text{O}$, and P_2O_5 in fused silica. The single-crystal X-ray diffraction shows that the title compound crystallizes in a triclinic ($P\bar{1}$) unit cell, with lattice dimensions $a = 6.145(2)$ Å, $b = 9.348(2)$ Å, $c = 6.009(1)$ Å, $\alpha = 96.46(2)^\circ$, $\beta = 100.16(2)^\circ$, $\gamma = 73.97(2)^\circ$, $V = 325.8(1)$ Å³; $Z = 4$. The structure has been refined by the least-squares method to $R = 0.019$, $R_w = 0.030$, and $\text{GOF} = 1.43$ for 128 variables. The four copper atoms in each asymmetric unit adopt three distorted coordination geometries that are consistent with the corresponding electronic states, e.g., square pyramidal $\text{Cu}(1)^{\text{II}}\text{O}_5$, octahedral $\text{Cu}(2)^{\text{II}}\text{O}_6$, and linear $\text{Cu}(3,4)^{\text{I}}\text{O}_2$. A low-dimensional framework exists consisting of arrays of nearly parallel CuO_2 units which are separated by the nonmagnetic, closed-shell P^{5+} cation in PO_4 tetrahedra. Closely spaced CuO_2 chains and a relatively short $\text{Cu}^{\text{I}}-\text{Cu}^{\text{I}}$ distance, e.g., 2.737 Å for $\text{Cu}(3)-\text{Cu}(3)$, are attributed to the bond strength of the cross-linked PO_4 tetrahedra. In the extended $\text{Cu}(I/II)-\text{O}$ framework, short linkages of $\text{Cu}^{\text{I}}-\text{O}-\text{Cu}^{\text{II}}-\text{O}-\text{Cu}^{\text{I}}$ and $\text{Cu}^{\text{II}}-\text{O}-\text{Cu}^{\text{II}}$, composed of regular $\text{Cu}-\text{O}$ bonds (1.86–1.99 Å), are interconnected through long $\text{Cu}^{\text{II}}-\text{O}$ bonds (2.36–2.74 Å). The magnetic measurements indicate that the $\text{Cu}-\text{O}$ framework exhibits a spin $1/2$ ground state and an antiferromagnetic ordering with a broad susceptibility maximum between 95 and 105 K. The results of stoichiometric synthesis, thermal analysis, and bond valence sum calculations of the title compound are also discussed.

Introduction

Our recent studies in the synthesis of mixed-valence, low-dimensional oxo compounds, e.g., the $\text{La}_4\text{Ti}(\text{Si}_2\text{O}_7)_2(\text{TiO}_2)_{4m}$ ($m = 1, 2$)¹ and $(\text{Ba}_3\text{Nb}_6\text{Si}_4\text{O}_{26})_n(\text{Ba}_3\text{Nb}_8\text{O}_{21})$ ($n = 1-4$) series,² have been insightful. In these examples, the fused transition metal oxide framework is structurally isolated and electronically insulated by nonmagnetic, closed-shell oxyanions, specifically $\text{Si}_2\text{O}_7^{6-}$. In the titanium series, the structures consist of (110) rutile sheets, in various thicknesses (m), that are separated by the silicate slab. To study the oxo chemistry associated with late transition metal oxides, we have extended our research into the copper phosphate³ and arsenate⁴ systems.

Most of the copper-based compounds reported so far are phosphates and silicates of copper(II) (see ref 3a and refs 6 and 7 therein). These compounds are unique in the sense that their structures contain distorted CuO_n ($n = 4, 5, 6$) polyhedra due to the electronic state of the Cu^{2+} (d^9) cation. The only electronically distinct compounds reported in the Cu-based systems are Cu(I) phosphate, CuPO_3 ,⁵ which has an unknown structure, and Cu(I/II) arsenate, $\text{Pb}_2\text{Cu}_8(\text{AsO}_4)_6$.⁶

To explore copper(I/II) oxophosphate compounds, a phase compatibility study of the $\text{Cu}_2\text{O}-\text{CuO}-\text{P}_2\text{O}_5$ system ($\text{Cu/P} \geq 1.0$) has been initiated. It is known that the high-temperature chemistry of CuO is complicated by the instability of the cupric

ion, e.g., $2\text{CuO} \rightarrow \text{Cu}_2\text{O} + 1/2\text{O}_2$ at 1026 °C in air.⁷ The reaction temperatures were, therefore, set at 900 °C or below. A novel copper(I/II) phosphate was isolated, and the structure contains an interesting low-dimensional array of parallel $\text{Cu}^{\text{I}}\text{O}_2$ chains. The thermal and magnetic properties are also discussed.

Experimental Section

Synthesis. Dark brown single crystals of Cu_2PO_4 were grown from a stoichiometric mixture of $\text{Cu}_2\text{O}/\text{CuO}/\text{P}_2\text{O}_5$. In a typical reaction, 2.25 mmol of Cu_2O (Aldrich, 97%), 4.50 mmol of CuO (Aldrich, 99.99+%), and 2.25 mmol of P_2O_5 (Aesar, 99+%) were loaded in a N_2 purged drybox. This mixture was ground and then placed in a carbon-coated silica ampule, which was sealed under vacuum and double-jacketed in fused silica. The reaction was heated to 900 °C for 9 days and cooled at a rate of 9 °C/h to 500 °C and then 93 °C/h to room temperature. The yield was a mixture of Cu_2PO_4 , $\text{Cu}_3(\text{PO}_4)_2$, and Cu in 30%, 65%, and 5%, respectively, based on the intensity profiles of the powder X-ray diffraction (PXRD) pattern. Although the inner tube was severely attacked, no silicon was incorporated into the reaction products. Quantitative analysis by wavelength dispersive spectroscopy using a Cameca SX-50 was performed on the data crystal and showed two cationic elements Cu and P (no Si) with average weight percents of 61.17% and 13.87%, respectively, while oxygen was found to be 27.43%. These values are comparable with the calculated percents in Cu_2PO_4 , e.g., 57.2%, 13.9%, and 28.8%.

The stoichiometric synthesis was carried out after the structure determination, using the same procedures mentioned above. The maximum heating temperature for the best product was 500 °C. The bluish impurity phase, $\text{Cu}_3(\text{PO}_4)_2$, was always present in ca. 5%, on the basis of PXRD patterns. Fifteen indexed reflections were used in the program LATT,⁸ and the lattice constants were refined by least-squares method. The resulting dimensions are in good agreement with those from single-crystal indexing, e.g., $a = 6.150(3)$ Å, $b = 9.359(6)$ Å, $c = 6.013(3)$ Å, $\alpha = 96.47(5)^\circ$, $\beta = 100.08(6)^\circ$, $\gamma = 74.04(4)^\circ$, and $V = 326.3(3)$ Å³.

(7) Gadalla, A. M. M.; Ford, W. F.; White, J. *Trans. Brit. Ceram. Soc.* **1963**, 45, 62.

(8) LATT: Takusagawa, F. Ames Laboratory, Iowa State University, Ames, IA, unpublished research, 1981.

† Present address: Department of Chemistry, Clemson University, Clemson, SC 29634.

[⊗] Abstract published in *Advance ACS Abstracts*, September 1, 1995.

- (1) (a) Wang, S.; Hwu, S.-J. *J. Am. Chem. Soc.* **1992**, 114, 6920. (b) Wang, S.; Hwu, S.-J. *Inorg. Chem.* **1995**, 34, 166. (c) Wang, S.; Hwu, S.-J.; Paradis, J. A.; Whangbo, M.-H. *J. Am. Chem. Soc.* **1995**, 117, 5515. (d) Wang, S. Ph.D. Dissertation, Rice University, 1993.
- (2) (a) Serra, D. L.; Hwu, S.-J. *J. Solid State Chem.* **1992**, 101, 32. (b) Serra, D. L. Ph.D. Dissertation, Rice University, 1993.
- (3) (a) Etheredge, K. M. S.; Hwu, S.-J. *Inorg. Chem.* **1995**, 34, 1495. (b) Etheredge, K. M. S.; Hwu, S.-J. *Inorg. Chem.* **1995**, 34, 3123.
- (4) Wardojo, T. A.; Hwu, S.-J. *J. Solid State Chem.* **1995**, in press.
- (5) Ball, M. C. *J. Chem. Soc.* **1968**, 1113.
- (6) Effenberger, H. *J. Solid State Chem.* **1995**, 114, 413.

Table 1. Crystallographic Data^a for Cu₂PO₄

chem formula	Cu ₂ PO ₄	fw	222.06
<i>a</i> , Å	6.145(2)	space group	<i>P</i> $\bar{1}$ (No. 2)
<i>b</i> , Å	9.348(2)	<i>T</i> , °C	23
<i>c</i> , Å	6.009(1)	λ , Å	0.710 69
α , deg	96.46(2)	ρ_{calcd} , g cm ⁻³	4.527
β , deg	100.16(2)	linear abs	134.3
γ , deg	73.97(2)	coeff, cm ⁻¹	
<i>Z</i>	4	<i>R</i> ^b	0.019
		<i>R</i> _w ^c	0.030

^a The cell constants are refined in the triclinic crystal system. ^b $R = \sum[|F_o| - |F_c|]/\sum|F_o|$. ^c $R_w = [\sum w(|F_o| - |F_c|)^2/\sum w|F_o|^2]^{1/2}$.

Table 2. Positional and Equivalent Displacement Parameters for Cu₂PO₄

atom	<i>x</i>	<i>y</i>	<i>z</i>	<i>B</i> _{eq} ^a (Å ²)
Cu(1)	0.33487(7)	0.96023(5)	0.80504(7)	0.91(2)
Cu(2)	0.11423(8)	0.72540(4)	0.97207(7)	0.93(2)
Cu(3)	0.36573(8)	0.63980(5)	0.45320(7)	1.26(2)
Cu(4)	0.17876(8)	0.34319(5)	0.56604(7)	1.42(2)
P(1)	0.2983(1)	0.38431(9)	0.1184(1)	0.59(3)
P(2)	0.1901(1)	0.99887(9)	0.2848(1)	0.46(3)
O(1)	0.0524(4)	0.9024(2)	0.8029(4)	0.7(1)
O(2)	0.4606(4)	0.6973(3)	0.7651(4)	1.0(1)
O(3)	0.3527(4)	0.0233(3)	0.1328(4)	0.7(1)
O(4)	0.2799(4)	0.5535(2)	0.1460(4)	0.9(1)
O(5)	0.2518(4)	0.3252(3)	0.8772(4)	1.2(1)
O(6)	0.2605(4)	0.0514(3)	0.5261(4)	0.8(1)
O(7)	0.1842(4)	0.8358(2)	0.2589(4)	0.8(1)
O(8)	0.1125(4)	0.3567(3)	0.2457(4)	0.9(1)

^a Equivalent isotropic thermal parameters defined as $B_{\text{eq}} = (8\pi^2/3) \times \text{trace } U$.

Structure Determination. An irregularly-shaped crystal with dimensions 0.1 × 0.2 × 0.3 mm was selected for single-crystal X-ray structure determination. Indexing and intensity data collection were performed at room temperature on a Rigaku AFC5S four-circle diffractometer (Mo K α radiation) equipped with a graphite monochromator. The crystallographic data are tabulated in Table 1. The unit cell parameters and the orientation matrix for data collection were determined by a least-squares fit of 25 peak maxima, $8^\circ < 2\theta < 30^\circ$. A total of 1673 reflections ($2\theta_{\text{max}} = 55^\circ$) were collected at room temperature from four octants ($h, \pm k, \pm l$), of which 1480 reflections with $I > 3\sigma(I)$ were used for the structure solution. There was no detectable decay in intensity profiles according to three standard reflections (-5,-5,2; -4,-6,-1; 0,-9,0) which were measured every 150 reflections during data collection. Data reduction, intensity analysis, and extinction conditions were determined with the program PROCESS. The common centrosymmetric space group (*P* $\bar{1}$) was unambiguously chosen for the triclinic unit cell and was shown to be correct by subsequent structure solution and refinement. The TEXSAN software package⁹ was used for crystal structure solution and refinement. Lorentz polarization and empirical absorption corrections based on three computer-chosen azimuthal scans ($2\theta = 14.90, 28.86, \text{ and } 28.82^\circ$) were applied to the intensity data. The atomic coordinates were found by direct methods using SHELXS-86,¹⁰ which identified the positions of the copper and phosphorus atoms. The oxygen atoms were resolved using difference maps. The structural and thermal parameters were refined by full-matrix least-squares methods to $R = 0.019$, $R_w = 0.030$, and $\text{GOF} = 1.43$. Final positional and thermal parameters are listed in Table 2.

Thermal Analysis. Thermogravimetric (TGA) and differential thermal analysis (DTA) were carried out by a DuPont 9900 thermal analysis system in the temperature range 20–1000 °C. The experiments

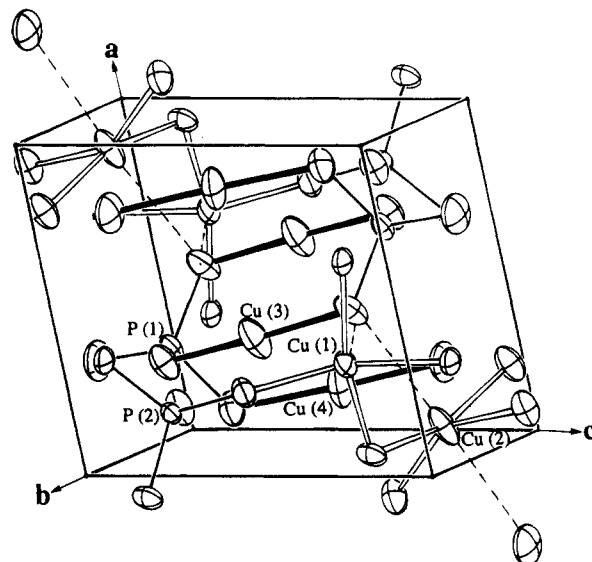


Figure 1. ORTEP drawing of the unit cell for Cu₂PO₄. The anisotropic thermal ellipsoids are drawn in 90% probability. The Cu(1)O₅ and Cu(2)O₆ coordination geometries are outlined by hollow and dotted lines representing short and long bonds, respectively; the Cu(3)O₂ and Cu(4)O₂ are represented by solid thick lines. The P(1)O₄ and P(2)O₄ coordination geometries are shown with thin lines.

were done on a ground powder of selected single crystals in an O₂ atmosphere. The TGA result suggests that the mixed-valence compound Cu₂PO₄ is subject to oxidative decomposition (based on PXRD) of Cu^I to Cu^{II} at ~315 °C. The corresponding weight gain is observed to be 3.69% vs the calculated value of 3.60%. The DTA result indicates that the title compound melted congruently at 571 °C and remained stable up to 1000 °C under vacuum. On the basis of the DTA experiment, it is tempting to say that, in the crystal growth reaction, Cu₂PO₄ formed at a high temperature, as high as 900 °C, and crystallized in cooling. Attempts to prepare single crystals from its own melt failed, however.

Magnetic Measurements. The magnetic susceptibility was measured by using a Quantum Design SQUID MPMS-5S magnetometer. The measurements were carried out from 1.76 to 300 K in fields of $H = 0.3, 0.7, 1, 3.5, \text{ and } 5 \text{ T}$. A powder sample (~31.2 mg) was contained in a gel capsule sample holder which was suspended in a straw from the sample translator drive. The temperature and field dependence of the susceptibility of the container were previously determined and their effect was negligible. The magnetic susceptibility was also corrected for paramagnetic impurities as well as core diamagnetism.

Results and Discussion

Structure Description. An ORTEP¹¹ drawing of the unit cell of Cu₂PO₄ is shown in Figure 1, where the coordination geometries of the copper and phosphorus cations with respect to the oxygen anions are highlighted. The structure, in terms of overall connectivity and chemical bonding, is complicated, as are most copper-based phosphates, due, in part, to the multiple coordination geometries of copper. In Cu₂PO₄, the copper coordinations can be approximated as a square-pyramidal Cu(1)O₅, an octahedral Cu(2)O₆, and a linear CuO₂ for both Cu(3) and Cu(4). The phosphorus atom has regular PO₄ tetrahedral coordination.

A fascinating feature, a low-dimensional array of CuO₂ chains, has been identified, which consists of Cu(3)O₂/Cu(4)O₂ units separated by layers of the phosphorus cation, P⁵⁺, in PO₄ tetrahedra, as shown in Figure 2. The structural composition, with respect to the copper atoms bonded to each PO₄, can be written as Cu_{4/2}PO₄ \equiv Cu₂PO₄. The Cu(3)O₂ and Cu(4)O₂

(9) (a) TEXSAN: Single Crystal Structure Analysis Software, Version 5.0, Molecular Structure Corp., The Woodlands, TX, 1989. (b) Cromer, D. T.; Waber, J. T. Scattering Factors for Non-hydrogen Atoms. In *International Tables for X-ray Crystallography*; Kynoch Press: Birmingham, England, 1974; Vol. IV, Table 2.2A, pp 71–98.

(10) Sheldrick, G. M. In *Crystallographic Computing 3*; Sheldrick, G. M., Krüger, C., Goddard, R., Eds.; Oxford University Press: London/New York, 1985; pp 175–189.

(11) Johnson, C. K. ORTEP II; Report ORNL-5138; Oak Ridge National Laboratory: Oak Ridge, TN, 1976.

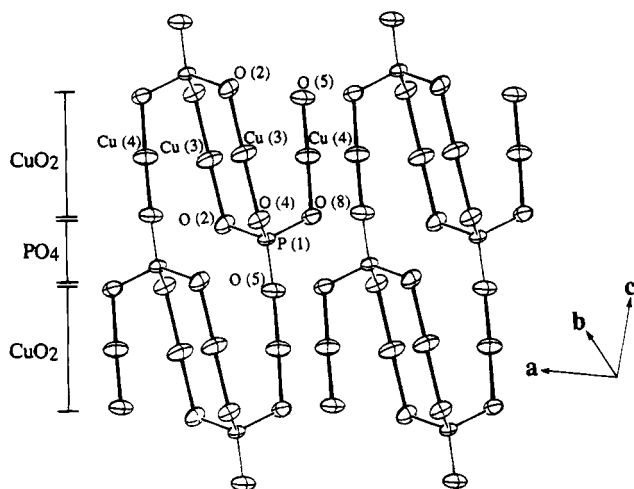


Figure 2. ORTEP drawing of the Cu₂PO₄ unit. The bond distances (Å) are 1.924(2), 1.973(2), 1.860(2), and 1.907(2) for Cu(3)–O(2), Cu(3)–O(4), Cu(4)–O(5), and Cu(4)–O(8), respectively. The P–O bonds are in the range of 1.50–1.57 Å.

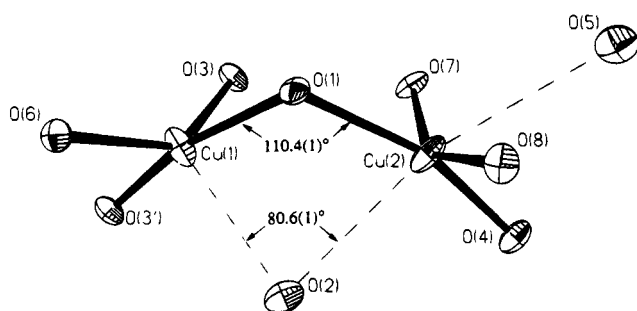


Figure 3. Double-polyhedral unit of edge-shared Cu(1)O₅ and Cu(2)O₆. The dotted lines represent long bonds, which are composed of the copper to apex oxygen atoms. The bond distances (Å) are as follows: Cu(1)O₅, 1.953(2), 1.984(2), 1.936(2), 1.892(2), and 2.363(2) for Cu(1)–O(1), O(3), O(3'), O(6), and O(2); Cu(2)O₆, 2 × 1.952(2), 1.950(2), 1.991(2), 2.588(2), and 2.740(2) for Cu(2)–O(1), O(4), O(7), O(8), O(2), and O(5), respectively.

units are distorted from a linear geometry with the bond angles of 172.4 (1) and 178.2 (1)°, respectively. These chains are nearly parallel and extend along the [100] direction. The Cu–O distances are in the range 1.86–1.97 Å, which is longer than 1.81 Å, the sum of Shannon crystal radii of 0.60 Å of two-coordinated Cu⁺ and 1.21 Å of two-coordinated O²⁻.¹² (A third bond, Cu(3)–O(7), is significantly longer, 2.204 (2) Å.) The lengthening of the Cu–O bond, compared to 1.89 Å in Pb₂Cu₈(AsO₄)₆,⁶ is likely due to the close interaction of parallel CuO₂ units that share the corner oxygens with the PO₄ tetrahedra stacking along the [001] direction. Closely spaced CuO₂ and a short Cu–Cu distance, e.g., 2.737 Å for Cu(3)–Cu(3), are attributed to the bond strength of the cross-linked PO₄ tetrahedra. This Cu–Cu distance is shorter than 2.857 and 2.876 Å in Cu^{II}₄(PO₄)₂O,¹³ where the short distances result from edge-shared CuO_n polyhedra, but is longer than 2.56 Å in copper metal.¹⁴

The double-polyhedral unit, shown in Figure 3,¹⁵ consists of Cu(1)O₅ and Cu(2)O₆ polyhedra that are distorted from an octahedral geometry. The two polyhedra share a common edge,

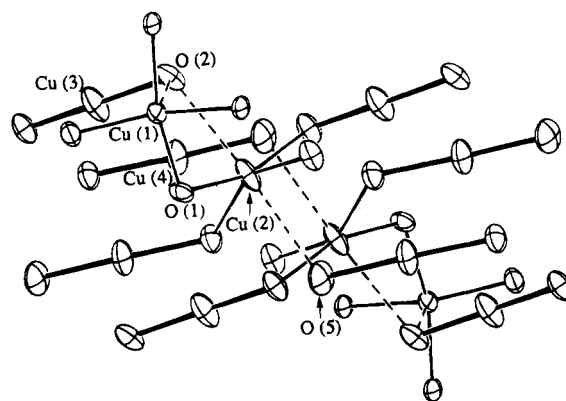


Figure 4. Viewed approximately along the same direction as in Figure 1, the Cu(I/II)–O framework is shown by the short bonds of the CuO₂ chain (thick lines) and the distorted square-planar CuO₄ (thin lines) of the Cu(1)O₅ and Cu(2)O₆ double-polyhedra. The dotted lines represent the long bonds of the double-polyhedra, e.g., Cu(1)–O(2) and Cu(2)–O(2,5).

O(1)–O(2). These polyhedra are made up of four regular bonds in buckled square planes with bond distances in the range 1.89–1.99 Å. This range is comparable with 1.93 Å, the sum of Shannon crystal radii of 0.71 Å of four-coordinated Cu²⁺ and 1.22 Å of three-coordinated O²⁻.¹² The apex oxygen atoms adopt considerably longer distances for both polyhedra, e.g., 2.36 Å for Cu(1)–O(2) and 2.59/2.74 Å for Cu(2)–O(2)/Cu(2)–O(5), and the bond angles for bridging oxygens, O(1) and O(2), are 110.4 (1) and 80.6 (1)°, respectively.

The oxygen atoms, O(1), O(2), and O(5), associated with the three long bonds, are shared between the CuO₂ array and the double-polyhedra unit. In the extended three-dimensional Cu(I/II)–O framework, as shown in Figure 4, short linkages of Cu^I–O–Cu^{II}–O–Cu^I and Cu^{II}–O–Cu^{II}, composed by short Cu–O bonds (1.86–1.99 Å), are interconnected through long Cu^{II}–O bonds (2.36–2.74 Å). O(2) is also shared within the double-polyhedra.

The above discussed coordination geometries of copper cations are consistent with the corresponding formal oxidation states derived from bond valence sum (BVS) calculations.¹⁶ The calculated charges for Cu(1) and Cu(2) are +2.14 and +2.01 including long bonds vs +1.98 and +1.87 excluding long bonds, respectively. This suggests that the formal oxidation state of each copper cation of the double-polyhedra can be assigned as +2. The structure distortion is expected due to the d⁹ electron configuration of the Cu²⁺ cation. Jahn–Teller distortion typically causes an elongation along the apex of the octahedral axis creating the situation seen here with four short equatorial Cu–O bonds and one or two long apical bonds. For Cu(3) and Cu(4), however, the calculated BVS values are +0.68 and +0.81, respectively, which are lower than +1, the expected oxidation state for a linear CuO₂ of Cu⁺ (d¹⁰). These resulting low values are, in part, due to the contribution from closely spaced CuO₂ array.¹⁷ The linear coordination, is also found in the above mentioned Pb₂Cu₈(AsO₄)₆ as well as copper(I) oxides, Cu₂O,¹⁸ CuFeO₂,¹⁹ and tetragonal YBa₂Cu₃O₆.²⁰

(12) Shannon, R. D. *Acta Crystallogr.* **1976**, A32, 751.

(13) (a) Brunel-Laügt, M.; Durif, A.; Guitel, J. C. *J. Solid State Chem.* **1978**, 25, 39. (b) Anderson, J. B.; Shoemaker, G. L.; Kostiner, E. J. *Solid State Chem.* **1978**, 25, 49.

(14) Greenwood, N. N.; Earnshaw, A. *Chemistry of the Elements*; Pergamon Press: Oxford, U.K., 1984; pp 1366–1368.

(15) SHELXTL PC VERS. 4.1, Siemens Crystallographic Research Systems, May 1990, Siemens Analytical X-ray Instruments Inc., Madison, WI.

(16) Brown, I. D.; Altermatt, D. *Acta Crystallogr.* **1985**, B41, 244.

(17) To carry out this analysis, the r_0 (1.55) value for Cu^I needs to be calculated by using Brown and Altermatt's algorithm. It should be noted that this value is considered to be "not as good" as the experimentally determined values according to ref 14.

(18) Wells, A. F. In *Structural Inorganic Chemistry*, 5th ed.; Oxford University Press: New York, 1984; p 127.

(19) Prewitz, C. T.; Shannon, R. D.; Rogers, D. B. *Inorg. Chem.* **1971**, 10, 719.

(20) Uimin, G.; Rossat-Mignod, J. *Physica C* **1992**, 199, 251.

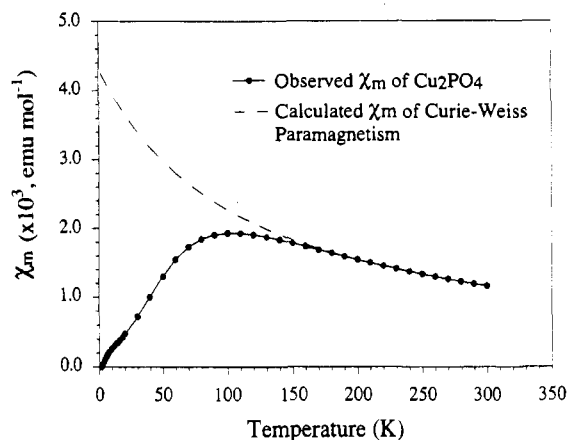


Figure 5. The molar susceptibility (χ_m) vs temperature (T , K) curve (solid dots and line) of Cu_2PO_4 . The dotted line indicates the Curie–Weiss behavior on the basis of the paramagnetic susceptibility above the Néel temperature, T_N .

Magnetic Properties. The mixed-valence copper(I/II) oxophosphate, Cu_2PO_4 , is antiferromagnetic with a broad susceptibility maximum between 95 and 105 K and a nearly zero interception at $T = 0$ K. This antiferromagnetic ordering temperature is field independent at $H = 0.3$ –5 T. Figure 5 shows the molar susceptibility (χ_m) vs temperature (T , K) curve of the title compound. A Curie tail was corrected according to a least-squares fit of $\chi = \chi_0 + C/(T - \Theta)$ at $T < 8$ K, where χ = measured susceptibility less $\chi(\text{anti})$ (emu mol^{-1}),²¹ χ_0 = sum of temperature-independent paramagnetic and diamagnetic susceptibilities²² ($1.80 \times 10^{-5} \text{ emu mol}^{-1}$), C = Curie constant ($6.22 \times 10^{-3} \text{ emu K mol}^{-1}$), and Θ = Weiss temperature (-3.04 K). The least-squares fit of the corrected magnetic data above the transition yields the magnetic moment of $1.67 \mu_B$, which is comparable with the spin-only ($S = 1/2$) value $1.73 \mu_B/\text{mol}$ of Cu_2PO_4 . The negative deviation from the Curie–Weiss plot, drawn in a dotted line, based on the curve fit of χ_m at $170 \text{ K} \leq T \leq 300 \text{ K}$, indicates an antiferromagnetic coupling with a broad transition temperature range. (The curvature existing at $T < 9$ K is likely due to the imperfect nature of the above said correction.) Antiferromagnetic coupling is likely induced via a commonly known superexchange mechanism²³

(21) The antiferromagnetic susceptibility, $\chi(\text{anti})$, at $T < 9$ K is acquired from the extrapolation of χ between 30 and 70 K. In this temperature range, the measured values are mostly due to antiferromagnetic ordering, assuming the paramagnetic contribution is comparably small.
 (22) O'Connor, C. J. *Prog. Inorg. Chem.* **1982**, 29, 203.

through the $\text{Cu}(1)\text{—O}(1)\text{—Cu}(2)$ pathway (Figure 3). Its angle, 110.4° , is greatly deviated from orthogonal, suggesting a $J < 0$ and a significant coupling between Cu(1) and Cu(2). A similar situation is seen in $\text{Cu}_4(\mu\text{-OCMe}_3)_6[\text{OC}(\text{CF}_3)_3]_2$.²⁴ This coupling is probably lowered due to the removal of electron density from the bridging oxygen by P^{5+} of the PO_4 group.

Summary

A novel mixed-valence copper(I/II) phosphate, Cu_2PO_4 , is isolated for the first time. The three-dimensional Cu–O framework is made of corner and edge-shared polyhedra. The complexity of the structure is attributed to the adaptive nature of distorted polyhedra, and the irregular bond interactions may be responsible for the observed low-melting behavior. Three types of distorted coordination geometries are seen that are consistent with the corresponding electronic states, e.g., square pyramidal $\text{Cu}(1)\text{O}_5$, octahedral $\text{Cu}(2)\text{O}_6$, and linear $\text{Cu}(3,4)\text{O}_2$. In spite of the complicated lattice, an interesting low-dimensional array of nearly parallel CuO_2 chains is identified. A short Cu–Cu separation is due to a cooperative bond interaction associated with the bond strength of cross-linked PO_4 tetrahedra. The magnetic measurements indicate that the Cu–O framework exhibits a spin 1/2 ground state and an antiferromagnetic ordering with a broad susceptibility maximum between 95 and 105 K. In spite of the rich structural chemistry, very few electronic properties have been reported in the copper-based phosphate systems; we anticipate more interesting magnetochemistry in this compound family.

Acknowledgment. Support of this work from the National Science Foundation (Grant DMR-9208529) is gratefully acknowledged. Funds for the Rigaku AFC5S diffractometer and the SQUID magnetometer by the National Science Foundation are acknowledged. The authors are indebted to the reviewer for useful references leading into the appropriate magnetic properties discussion and Mr. M. L. Pierson and Dr. J. C. Stormer, Jr., for microprobe analysis.

Supporting Information Available: Figures showing DTA and TGA results and tables of detailed crystallographic data, anisotropic thermal parameters, and bond distances and angles (6 pages). Ordering information is given on any current masthead page.

IC950506W

(23) Hay, P. J.; Thibault, J. C.; Hoffmann, R. *J. Am. Chem. Soc.* **1975**, 97, 4884.
 (24) Purdy, A. P.; George, C. F.; Brewer, G. A. *Inorg. Chem.* **1992**, 31, 2633.